In situ resistivity measurements during the atomic layer deposition of ZnO and W thin films

M. Schuisky, J. W. Elam, and S. M. George

Citation: Applied Physics Letters **81**, 180 (2002); doi: 10.1063/1.1490413
View online: http://dx.doi.org/10.1063/1.1490413
View Table of Contents: http://scitation.aip.org/content/aip/journal/apl/81/1?ver=pdfcov
Published by the AIP Publishing

APPLIED PHYSICS LETTERS VOLUME 81, NUMBER 1 1 JULY 2002

In situ resistivity measurements during the atomic layer deposition of ZnO and W thin films

M. Schuisky and J. W. Elam
Department of Chemistry and Biochemistry, University of Colorado, Boulder, Colorado 80309-0215

S. M. George[a)]
Department of Chemistry and Biochemistry and Department of Chemical Engineering, University of Colorado, Boulder, Colorado 80309-0215

(Received 4 March 2002; accepted for publication 6 May 2002)

In situ monitoring of the electrical resistivity of ZnO and W thin films during atomic layer deposition (ALD) was performed using a four-point probe. Large oscillations were observed during the ZnO ALD resistivity measurements. The resistivity dramatically increased during each diethyl zinc exposure and decreased during each H_2O exposure. In contrast, the W ALD resistivity measurements exhibited a steplike pattern where the resistivity decreased during the Si_2H_6 exposures and remained constant during the WF_6 exposures. *In situ* resistivity measurements will be useful to monitor ALD processing and also may help to optimize and understand the properties of gas sensors. © *2002 American Institute of Physics.* [DOI: 10.1063/1.1490413]

Atomic layer deposition (ALD) is a growth technique allowing highly conformal films to be deposited with atomic level thickness control.[1,2] ALD is a variant of chemical vapor deposition (CVD). In ALD, a binary CVD reaction is divided into two self-limiting half reactions.[3] By repeating these half reactions in an *ABAB*... binary sequence, a thin film can be deposited one atomic layer per *AB* cycle.

The sequential nature of ALD allows each half reaction to be examined independently during film growth. However, typical ALD growth conditions challenge traditional surface science techniques. ALD is often performed under viscous flow at pressures of 1–10 Torr and using *AB* cycle times of only a few seconds. Nevertheless, a number of *in situ* techniques have been implemented to explore surface chemistry and growth during ALD including quadrupole mass spectrometry,[4] optical reflectivity,[5] and quartz crystal microbalance measurements.[6,7]

In this letter, we report the application of *in situ* resistivity techniques to monitor ALD. *In situ* resistivity measurements provide an excellent method for probing conductance changes during thin-film growth.[8,9] The electrical resistivity of thin films is determined by both bulk and surface effects. Electrical resistivity is influenced by electron scattering from phonons, point defects, impurities, and grain boundaries.[10] For film thicknesses less than the electron mean-free path, the resistivity increases because of interfacial scattering. The resistivity can also be influenced dramatically by adsorbed species that alter charge carrier concentrations or intergranular barrier heights.[11]

In situ resistivity measurements typically employ a four-point probe that is brought into contact with the substrate.[12] This method allows resistivity measurements at discrete thickness intervals after particular deposition times. To enable continuous *in situ* resistivity monitoring, a special device was designed that integrated the four-point probe with the deposition substrate. A $5\times5\ \mathrm{mm}^2$ alumina substrate was lithographically patterned with gold as shown in Fig. 1(a). The four-point probe consisted of four $50\times50\ \mu\mathrm{m}^2$ gold contacts in a symmetric van der Pauw geometry separated diagonally by 1 mm. Gold lines with a width of 25 μm connected the contacts to $1\times1\ \mathrm{mm}^2$ gold pads at the edges of the substrate.

A constant current, I, was applied through contacts A and B and the resulting voltage difference, V, was measured between contacts C and D. For symmetrical, circular, or square probe geometries, the resistivity, ρ, is calculated from[13]

$$\rho=4.532Rd, \tag{1}$$

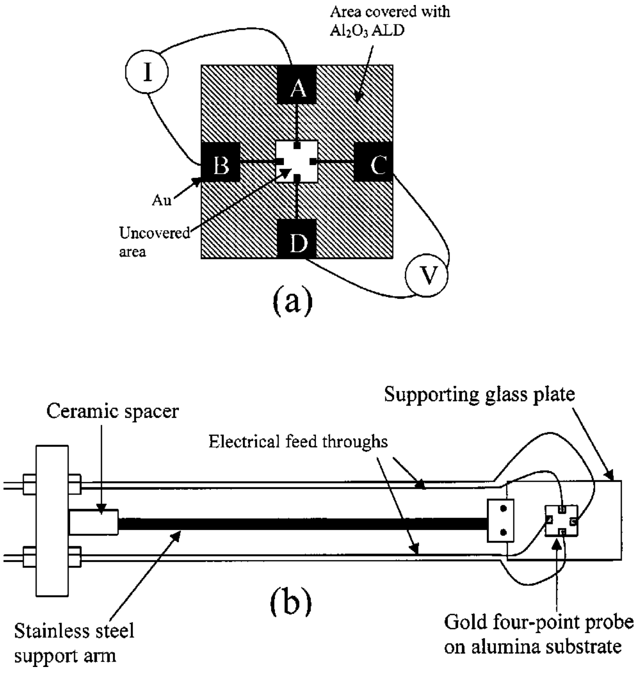

FIG. 1. Schematic diagram of (a) the gold four-point probe deposited on the alumina substrate and (b) the four-point probe mounted on the conflat flange.

[a)] Electronic mail: steven.george@colorado.edu where $R=V/I$ is the resistance between contacts C and D and d is the film thickness. The film thicknesses were determined using previously derived growth rates.

The ceramic substrate was glued to a supporting glass plate that was clamped at the end of a stainless-steel arm as shown in Fig. 1(b). The four-point probe was mounted to a 2.75 in. conflat flange equipped with four electrical feedthroughs. The gold pads were connected to the electrical feedthroughs using 0.05 mm diameter wires. The *in situ* four-point probe was then installed in a viscous flow ALD reactor.[14]

To prevent the electrical shorting or grounding of the four-point probe by the conducting ALD films, the stainless-steel arm was isolated using a ceramic spacer. In addition, a flow of nitrogen gas purged the inside surface of the conflat flange. The four-point probe was also coated with an insulating Al_2O_3 ALD layer. Photoresist was initially placed over the $50\times 50\ \mu m^2$ gold contacts. Al_2O_3 ALD was then performed using 800 trimethyl aluminum/H_2O cycles at 177 °C to deposit an insulating Al_2O_3 layer with a thickness of ~100 nm.[15] The photoresist was subsequently removed with acetone to expose the $50\times 50\ \mu m^2$ gold contacts.

ZnO ALD films were grown using diethyl zinc (DEZ) and water at 177 °C with exposure times of 1 s and purge times of 5 s. Under these conditions, the ZnO ALD growth rate is $2.01(\pm 0.01)$ Å/*AB* cycle. Figure 2(a) shows the four-point probe voltage measurements versus deposition time. The voltage measurements commence at ZnO *AB* cycle number 89 at a film thickness of $179(\pm 1)$ Å. The measurements continued until 200 AB cycles when the ZnO film is 402 (± 4) Å thick. At 1550 s, the constant current was increased by a factor of 100 to compensate for the decreasing resistance and the measured voltage was subsequently divided by 100.

Figure 2(a) demonstrates that the resistance of the ZnO ALD film decreases with increasing thickness. By applying Eq. (1) and the known ZnO ALD growth rate, Fig. 2(a) yields a resistivity at 177 °C that drops from an initial value of 0.1 Ω cm to a limiting value of ~0.002 Ω cm. This limiting value is slightly lower than the bulk resistivity value of ~0.008 Ω cm determined by *ex situ* four-point probe measurements under ambient conditions at room temperature. A lower resistivity value at 177 °C is expected because the resistivity of the ZnO semiconductor film should decrease with increasing temperature. The ZnO film resistivity may also increase upon air exposure.

The voltage measurements in Fig. 2(a) also exhibit pronounced oscillations. Figure 2(b) shows an expanded view of the corresponding resistivity values for *AB* cycles 89–92. The resistivity increases dramatically during each DEZ exposure and subsequently drops with the next H_2O exposure. Oscillations in the resistivity of thin metallic films have previously been explained as resulting from either periodic roughness changes or quantum size effects.[9,16] These explanations are unlikely in the current experiment.

The resistivity oscillations may reflect changes in conductance because of the adsorbed species. The adsorbed chemical groups may act as electron donors or acceptors and change the charge carrier concentration in the ZnO film. Alternatively, the adsorbed chemical groups may alter the conduction barrier heights at intergranular contacts.[11] The DEZ vapor will react with surface hydroxyl groups according to[7]

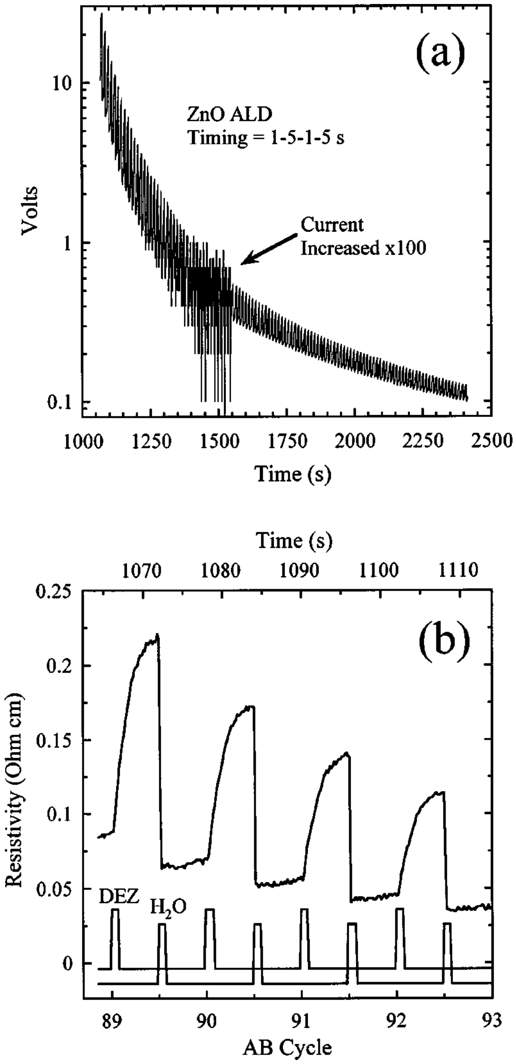

FIG. 2. (a) Voltage versus time measured using the *in situ* four-point probe during ZnO ALD. (b) Expanded view of the resistivity values vs ZnO *AB* cycle.

$$ZnOH^* + Zn(CH_2CH_3)_2 \rightarrow ZnOZnCH_2CH_3^* + CH_3CH_3, \tag{2}$$

where the asterisks denote surface species. The large increase in resistivity upon DEZ exposure is associated with the conversion of surface hydroxyl groups into alkyl species by the covalent attachment of Zn–alkyl groups. The second half reaction proceeds by[7]

$$ZnOZnCH_2CH_3^* + H_2O \rightarrow ZnOZnOH^* + CH_3CH_3. \tag{3}$$

Reaction 3 will restore the initial hydroxyl surface groups and deposit additional ZnO. The resistivity subsequently drops below the resistivity value measured before the ALD cycle.

Additional *in situ* resistivity measurements explored W ALD. The W ALD was performed using tungsten haxafluoride (WF_6) and disilane (Si_2H_6) exposures of 2 s and purge times of 5 s at 300 °C. These conditions yield a W ALD growth rate of $5.5(\pm 0.1)$ Å/*AB* cycle. Figure 3(a) shows the *in situ* four-point probe voltage measurements versus the W

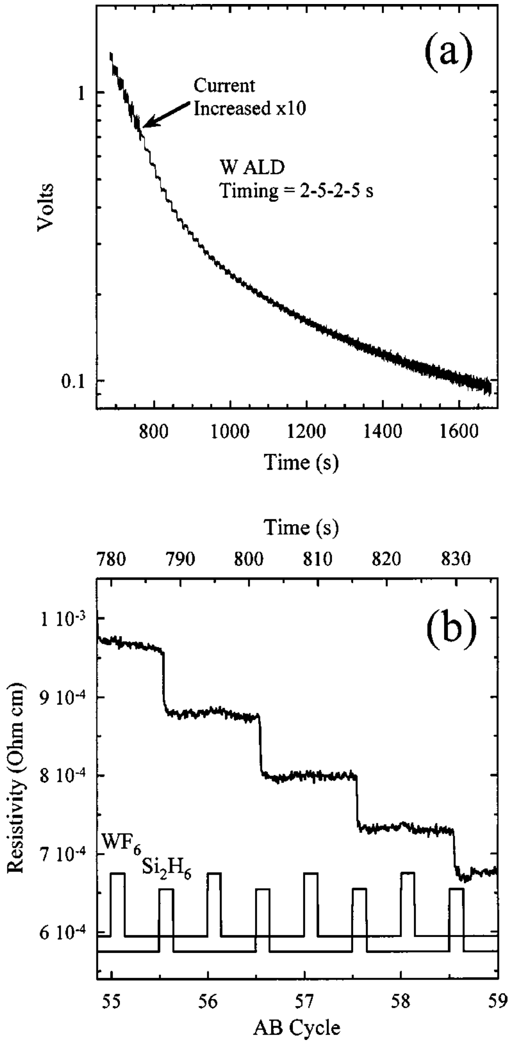

FIG. 3. (a) Voltage versus time measured using the *in situ* four-point probe during W ALD. (b) Expanded view of the resistivity values vs W *AB* cycle.

ALD growth time. The voltage measurements commence at W *AB* cycle 50 at a film thickness of 275(±5) Å. The four-point probe voltage is monitored for an additional 70 AB cycles until the W film is 660(±12) Å thick. During this interval, the W film resistivity at 300 °C dropped from $1.8 \times 10^{-3}\ \Omega\,\mathrm{cm}$ to $2.9 \times 10^{-4}\ \Omega\,\mathrm{cm}$. *Ex situ* resistivity measurements at ambient conditions at room temperature yielded a lower resistivity of $1.2 \times 10^{-4}\ \Omega\,\mathrm{cm}$ for a film thickness of 320 Å.[17] The slightly higher resistivity at 300 °C is expected because the resistivity of the W metallic film should increase with increasing temperature.

Figure 3(a) shows a distinct, stepped structure in the probe voltage. An expanded view of the corresponding resistivity values for *AB* cycles 55–59 is displayed in Fig. 3(b). The W film resistivity remains constant during the WF_6 exposures but drops rapidly during each Si_2H_6 exposure. This behavior indicates that the resistivity does not change when W is deposited as WF_x^* surface species during the WF_6 exposures according to the following half reaction[17]

$$WSiH_yF_z^* + WF_6(g) \rightarrow WWF_x^* + SiH_aF_b(g) + cH_2(g). \tag{4}$$

In contrast, a discrete drop in resistivity occurs when the subsequent Si_2H_6 exposure converts the WF_x^* surface species to metallic W atoms[17]

$$WF_x^* + Si_2H_6(g) \rightarrow WSiH_yF_z^* + SiH_aF_b(g) + dH_2(g). \tag{5}$$

The Si_2H_6 exposures also deposit $SiH_yF_z^*$ surface species. These functional groups must not influence the film conductance because their replacement by WF_x^* surface species during the following WF_6 exposure does not change the resistivity.

In conclusion, we report the application of *in situ* resistivity measurements to monitor the ALD of both semiconducting ZnO and metallic W thin films. Oscillations in the thin-film resistivity were observed that correspond to the ALD reactant pulse sequence. During ZnO ALD, the ethyl-terminated ZnO film displayed a much higher resistivity than the hydroxyl-terminated film. During W ALD, the resistivity only decreased when the fluorinated tungsten surface species were converted to metallic tungsten during the Si_2H_6 exposure. These results demonstrate that *in situ* resistivity measurements will be valuable to probe ALD surface chemistry and film growth. These results may also have important consequences for the understanding of thin film electrical properties and the development of gas sensors.

This research was supported by the National Science Foundation through grant CHE-9905812. The authors thank Nils Hoivik and Ryan Linderman at the Department of Mechanical Engineering, University of Colorado at Boulder for the design and construction of the four-point probes. One of the authors (M.S.) acknowledges the Wenner–Gren Foundations and the Sweden–America Foundation for financial support.

[1] T. Suntola, Thin Solid Films **216**, 84 (1992).
[2] M. Ritala and M. Leskelä, in *Handbook of Thin Film Materials*, edited by H. S. Nawa (Academic, San Diego, 2001).
[3] S. M. George, A. W. Ott, J. W. Klaus, J. Phys. Chem. **100**, 13121 (1996).
[4] M. Juppo, A. Rahtu, M. Ritala, and M. Leskelä, Langmuir **16**, 4034 (2000).
[5] A. Rosental, P. Adamsom, A. Gerst, H. Koppel, and A. Tarre, Appl. Surf. Sci. **112**, 82 (1997).
[6] J. Aarik, A. Adla, T. Uustare, M. Ritala, and M. Leskelä, Appl. Surf. Sci. **161**, 385 (2000).
[7] E. B. Yousfi, J. Fouache, and D. Lincot, Appl. Surf. Sci. **153**, 223 (2000).
[8] H.-D. Liu, Y.-P. Zhao, G. Ramanath, S. P. Murarka, and G.-C. Wang, Thin Solid Films **384**, 151 (2001).
[9] M. Jalochowski and E. Bauer, Phys. Rev. B **37**, 8622 (1988).
[10] D. Schumacher, *Surface Scattering Experiments with Conduction Electrons* (Springer, Berlin, 1993).
[11] A. Vancu, R. Ionescu, and N. Bârsan, in *Thin Film Resistive Sensors*, edited by P. Ciureanu and S. Middelhoek, (IOP, New York, 1992), Chap. 6.
[12] C. G. Wiegenstein and K. H. Schulz, Rev. Sci. Instrum. **68**, 1812 (1997).
[13] D. K. Schroder, *Semiconductor Material and Device Characterization* (Wiley, New York, 1998).
[14] J. W. Elam, M. D. Groner, and S. M. George, Rev. Sci. Instrum. (to be published).
[15] A. W. Ott, J. W. Klaus, J. M. Johnson, and S. M. George, Thin Solid Films **292**, 135 (1997).
[16] G. Palasantzas, Y. P. Zhao, G. C. Wang, T. M. Lu, J. Barnas, and J. T. M. De Hosson, Phys. Rev. B **61**, 11109 (2000).
[17] J. W. Klaus, S. J. Ferro, and S. M. George, Thin Solid Films **360**, 145 (2000).